ELSEVIER

Journal of Photochemistry and Photobiology A: Chemistry 135 (2000) 91–102

Journal of Photochemistry and Photobiology A:Chemistry

www.elsevier.nl/locate/jphotochem

Nitric oxide chemiluminescence enhancement by substituted benzenes

Stacey Noel Henegar, Hai Bui, S. Fowler Bush, Wade N. Sisk*

Chemistry Department, University of North Carolina at Charlotte, 9201 University City Blvd., Charlotte, NC 28223-0001, USA

Received 9 December 1998; received in revised form 8 March 2000; accepted 17 April 2000

Abstract

Enhancement of NO($A^2\Sigma^+ \rightarrow X^2\Pi$) chemiluminescence is reported for the 532-nm irradiation of an HC/NO_2 mixture, where HC is toluene, ethylbenzene, or xylene. Evidence is presented for the HC triplet state playing a key role in enhancing the fluorescence. The rate constants for production of NO($A^2\Sigma^+$) were determined as well as the quenching rate constants for each hydrocarbon. Using the latter, the NO($A^2\Sigma^+$) depletion rate constants were calculated for each reaction mixture. From this data, the nascent NO($A^2\Sigma^+$) yields were determined and compared to the observed chemiluminescence yields. Little difference was observed between the chemiluminescence yields for each of the hydrocarbons. However, comparison of the nascent NO($A^2\Sigma^+$) yields showed an increase for the xylenes that was twice that of benzene, toluene, or ethylbenzene. The lower formation rate constants and higher chemiluminescence/$[NO(A)]_0$ yields for the xylenes are explained by differences in the details of NO(A) production. The triplet-state argument is bolstered by the observation of NO($A^2\Sigma^+$) chemiluminescence following the focused 532-nm irradiated mixture of NO_2 and acrylaldehyde.

Keywords: Chemiluminescence; Hydrocarbons; Xylenes; Nitrogen oxides; Triplet state; Flourescence; Quenching

1. Introduction

1.1. Background

Nitric oxide chemiluminescence, following visible laser irradiation of gaseous mixtures, has been studied previously by Fujimura et al. [1] for neat NO_2 and by Sisk et al. [2] for NO_2/hydrocarbon mixtures. Two different mechanisms were proposed for the observed chemiluminescence in each case. Fujimura et al. [1] observed electronically excited NO following the ultraviolet multiphoton photolysis of neat NO_2 in which O(^{1}D) was an intermediate. The mechanism cited as producing excited NO is referred to herein as the *neat mechanism*:

$$NO_2 + h\nu \rightarrow NO_2(^2B_2) \quad (1)$$

$$NO_2 + nh\nu \rightarrow O(^1D) + NO \quad (2)$$

$$O(^1D) + NO_2(^2B_2) \rightarrow NO(A^2\Sigma^+) + O_2 \quad (3)$$

Absorption of multiple visible photons by NO_2 ultimately results in the production of electronically excited NO($A^2\Sigma^+$), which relaxes to the ground state. Absorption of one photon results in the excitation of NO_2 (Eq. (1)) while multiphoton absorption causes it to dissociate and produce excited monatomic oxygen and ground-state nitric oxide (Eq. (2)). These two products from Eqs. (1) and (2) react to form excited nitric oxide and molecular oxygen (Eq. (3)). In this reaction scheme, the reaction can be monitored by observing the NO($A^2\Sigma^+ \rightarrow X^2\Pi$) emission.

A related reaction scheme was proposed by Sisk et al. [2] involving NO_2 and a hydrocarbon that possesses a low-lying triplet state. Thus, this mechanism will be termed the *triplet mechanism*. This reaction scheme involves secondary absorption of a photon by a $NO_2(^2B_2)$/hydrocarbon complex resulting in the production of the hydrocarbon in the T_1 state. Two different pathways for the production of these species were proposed.

In the first pathway, (Eqs. (4)–(6)),

$$NO_2 + h\nu \rightarrow NO_2(^2B_2) \quad (4)$$

$$NO_2(^2B_2) + HC(+M) \leftrightarrow [NO_2 \cdots HC]^*(+M) \quad (5)$$

$$[NO_2 \cdots HC]^* + h\nu \rightarrow [NO_2 \cdots HC]^{**} \rightarrow NO_2 + HC^*(T_1) \quad (6)$$

In this mechanism, NO_2 absorbs one visible photon and is promoted to an electronic excited state (Eq. (4)). Excited

* Corresponding author. Tel.: +1-704-547-4433; fax: +1-704-547-3151.
E-mail address: wsisk@email.uncc.edu (W.N. Sisk)

1010-6030/00/$ – see front matter
PII: S1010-6030(00)00300-2

NO_2 then forms a complex with the ground-state hydrocarbon while possessing the energy of one visible photon. The hydrocarbon makes use of the large oscillator strength of NO_2 to absorb a second visible photon producing an excited NO_2/hydrocarbon complex, $[NO_2 \cdots HC]^{**}$, possessing the energy of two visible photons. This complex, subsequently, dissociates into ground-state NO_2 and triplet-state hydrocarbon as indicated in Eq. (6).

The second path by which the hydrocarbon may be excited to its triplet state is via the initial formation of a ground state NO_2-hydrocarbon complex, Eq. (7), which absorbs two visible photons, Eq. (8). Again, this excited complex dissociates yielding ground state NO_2 and triplet state hydrocarbon, Eq. (9). As before, the hydrocarbon makes use of the large oscillator strength of NO_2 to make the forbidden transition to the triplet state:

$$NO_2 + HC(+M) \leftrightarrow NO_2 \cdots HC(+M) \tag{7}$$

$$NO_2 \cdots HC + 2h\nu \rightarrow [NO_2 \cdots HC]^{**} \tag{8}$$

$$[NO_2 \cdots HC]^{**} \rightarrow NO_2 + HC^*(T_1) \tag{9}$$

Electronically excited NO_2 is produced by the absorption of a single visible photon Eq. (10) and subsequent relaxation to high vibrational levels of the ground electronic state Eq. (11):

$$NO_2 + h\nu \rightarrow NO_2(^2B_2) \tag{10}$$

$$NO_2(^2B_2) + M \rightarrow NO_2^{(*)} + M \tag{11}$$

Finally, in the last step(s) of the reaction sequence, vibrationally excited NO_2, and electronically excited hydrocarbon react (Eq. (12)) to form excited nitric oxide and oxidized hydrocarbon. The excited nitric oxide returns to the ground state via UV emission, Eq. (13):

$$HC^*(T_1) + NO_2^{(*)} \rightarrow NO(A^2\Sigma^+) + (\text{oxidized HC}) \tag{12}$$

$$NO(A^2\Sigma^+) \rightarrow NO(X^2\Pi) + h\nu \tag{13}$$

Thus, in comparison with the neat mechanism, the addition of the hydrocarbon to NO_2 leads to an enhancement of the NO fluorescence intensity following visible excitation. In the previous experiments by Sisk et al. [2], the photon energy was such that two-photon absorption was incapable of directly exciting the hydrocarbon to the S_1 state. Instead, the focused irradiation resulted in two-photon excitation of $[NO_2 \cdots HC]$ complex (Eq. (8)). Energy transfer from this complex to the hydrocarbon led to significant HC triplet-state populations. The triplet state of the hydrocarbon was credited for enhancing the nitric oxide fluorescence. The hydrocarbons noted to enhance the chemiluminescence are acetylene, methylacetylene, ethylacetylene, phenylacetylene, and benzene. The triplet states of these are energetically accessible by two visible photons.

Other species which exhibit the capability to enhance the NO chemiluminescence possessing similar energetics as the compounds studied previously would tend to further support the involvement of the low-lying triplet state of the hydrocarbons. In this report, NO chemiluminescence is measured for toluene, ethylbenzene, xylene and acrylaldehyde. The effect of steric factors will be determined by comparing the enhancement for the xylene isomers.

1.2. Kinetics

Consider the production and depletion of $NO(A^2\Sigma^+)$ by the following generic reaction scheme:

$$\text{REACTANT} \xrightarrow{k_1} NO(A^2\Sigma^+) \tag{14}$$

$$NO(A^2\Sigma^+) \xrightarrow{k_2} \text{PRODUCT} \tag{15}$$

The two reaction rate constants, k_1 in Eq. (14) and k_2 in Eq. (15), are the formation and depletion rate constants, respectively. Straightforward kinetics considerations lead to the following expression for the concentration of $NO(A^2\Sigma^+)$:

$$[NO(A^2\Sigma^+)] = \frac{(\text{const.})k_1\{e^{-k_1 t} - e^{-k_2 t}\}}{k_2 - k_1} \tag{16}$$

With the partial pressures utilized in these experiments $k_2 \gg k_1$, and the equation reduces to:

$$[NO(A^2\Sigma^+)] = (\text{const.}')e^{-k_1 t} \tag{17}$$

Using this relation, the data can be fitted to a single exponential function to determine the formation rate of $NO(A^2\Sigma^+)$. Note that k_1, the formation rate constant, is the *apparent* decay rate constant.

Another feature of interest is the chemiluminescence yield of $NO(A^2\Sigma^+)$ for a given mixture of NO_2 and hydrocarbon. The chemiluminescence yield, Φ_{LLC}, is proportional to the time-integrated concentration of $NO(A^2\Sigma^+)$:

$$\Phi_{LLC} \propto \int_0^\infty [NO(A^2\Sigma^+)]\,d\tau \tag{18}$$

In this equation, the subscript LLC designates the long-lived chemiluminescence attributed to the triplet mechanism. Experimentally, Φ_{LLC} values are determined by integrating the fluorescence temporal decay profiles.

2. Experimental

2.1. Chemiluminescence measurements

In these studies, a cell containing a mixture of NO_2 and the selected hydrocarbon is irradiated by 532-nm light, and the resulting UV emission observed. The apparatus for performing the chemiluminescence experiments, shown in Fig. 1, is similar to that used previously by Sisk et al. [2]. A Continuum Surelite I model Nd:YAG laser produces 532-nm radiation with 200 mJ/pulse. The laser was focused

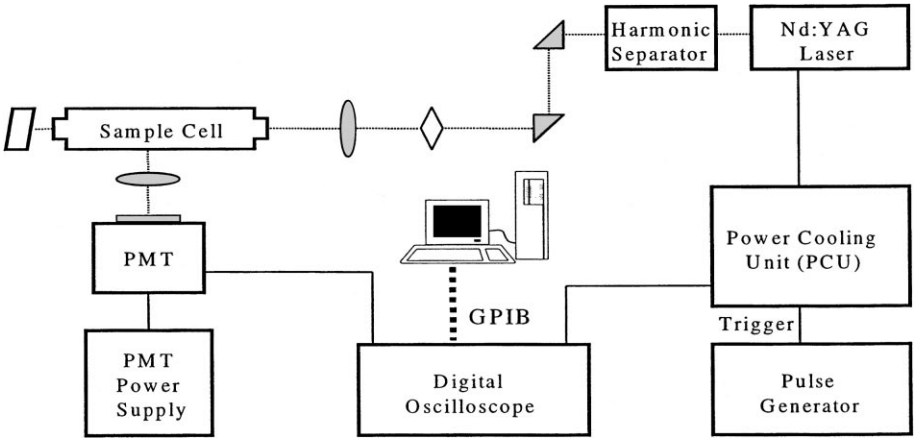

Fig. 1. NO_2 chemiluminescence experimental set-up.

by an *f*/4 lens in a glass cell equipped with suprasil windows, such that the emitted fluorescence was detected perpendicular to the beam path. A 2-in. diameter *f*/1 quartz lens focused the emitted fluorescence onto a Hamamatsu R166 model photomultiplier tube (PMT) equipped with a Corning 7–54 band-pass filter (200–350 nm) or onto the entrance slit of a 0.25-m PTI monochromator in order to observe the dispersed fluorescence. The PMT output was monitored using a LeCroy 9350 digital oscilloscope sampling at 1 Gs/s for temporal decays or monitored by an SRS boxcar integrator for dispersed fluorescence. Finally, the oscilloscope and boxcar signals were transferred to a computer via GPIB.

2.2. Quenching studies

In these studies, flourescence is monitored for the direct excitation of nitric oxide hydrocarbon mixtures via 226 nm photons. The set-up for performing the fluorescence quenching studies is similar to that used for the chemiluminescence experiments, except for changes in the excitation source. The Nd:YAG laser was converted to the third harmonic to produce light with a wavelength of 355 nm. This was used to pump a Continuum ND6000 dye laser supplied with Coumarin 450 laser dye. The dye laser was tuned to 452 nm, energetically equal to one-half the desired NO transition energy. A β-barium borate (BBO) crystal was used to double the 452-nm frequency light to 226 nm. No focusing optics were placed between the BBO crystal and the sample cell in an effort to discourage multiphoton absorption. The detection and data acquisition scheme were the same as those used in the chemiluminescence studies.

In order to prepare each sample mixture, 200 mTorr of nitric oxide was placed into the sample cell. The pressure of the sample cell was monitored directly using an MKS capacitance manometer. Once nitric oxide was placed into the cell, the vacuum manifold and transfer line were evacuated while the pressure was measured by a thermocouple gauge. A hydrocarbon was then expanded to the vacuum manifold and transfer line. A needle valve, used to regulate the addition of hydrocarbon to the sample cell, was placed between the transfer line and the sample cell. While using the large backing pressure of the hydrocarbon to prevent loss of nitric oxide into the vacuum system, the needle valve was opened to add an amount of hydrocarbon. The gases were then allowed to mix and equilibrate in the sample cell before triggering the laser. For each hydrocarbon, the desired amounts to be added (measured in mTorr) were 75, 150, 300, 400, 500, and 600. Also, one sample consisted of nitric oxide in the absence of any hydrocarbon. For each gas, the signal (scattered light) resulting from the 226-nm excitation of an evacuated cell was obtained. This evacuated cell signal was subtracted from the fluorescence signal to remove the scattered light contribution to the fluorescence.

2.3. Dispersed fluorescence

The apparatus used to observe the dispersed fluorescence was similar to the arrangement employed for the chemiluminescence studies. The observed fluorescence was dispersed using a 0.25 m PTI Czerny–Turner configured monochromator with 600 mm^{-1} ruled gratings. Slit widths varied but all spectral resolution is expected to be ≈2 nm throughout the observed spectral range. A computer-controlled stepper motor moved the grating of the monochromator in 1-nm intervals. At each interval, the laser was triggered 30 times at 10 Hz while the PMT signal was integrated using a Stanford Research Systems boxcar integrator.

The NO_2 was obtained from Charlotte Welding Supply and purified by several freeze-pump-thaw cycles to remove impurities. All the hydrocarbons used were obtained from department stock and are reagent grade. These were purified by performing several single-trap freeze-pump thaw cycles. Nitric oxide was obtained from Aldrich (stated purity, 99.9%) was used with no further purification.

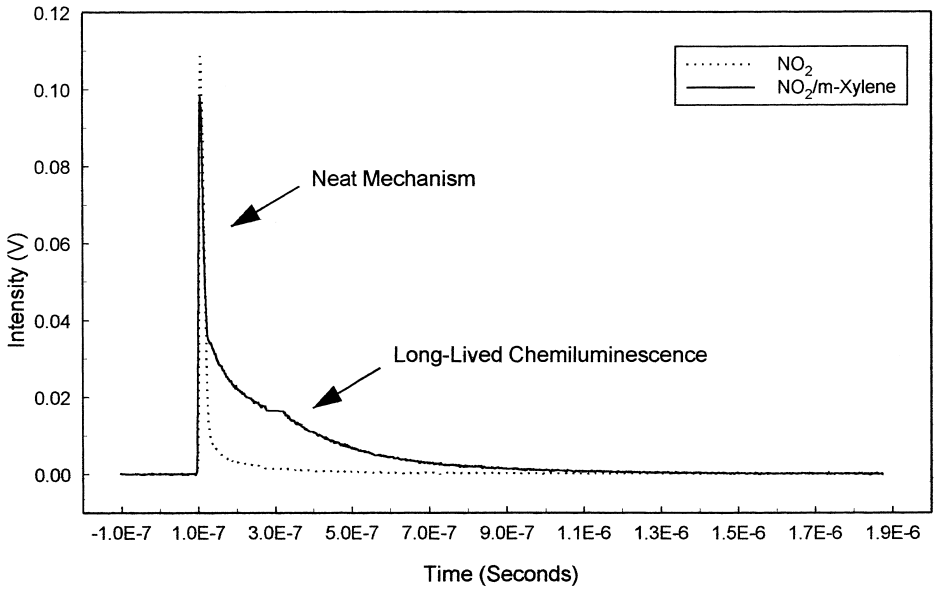

Fig. 2. Decay profile for 10-Torr NO_2 and 4-Torr *m*-xylene.

3. Results and discussion

3.1. Chemiluminescence

For each of the hydrocarbons considered, an enhancement of the chemiluminescence intensity for the HC/NO_2 mixture was observed relative to neat NO_2 (10 Torr). A typical fluorescence decay profile that illustrates the fluorescence enhancement is shown in Fig. 2 where the chemiluminescence signal from NO_2/*m*-xylene is superimposed upon the neat NO_2 signal in an effort to illustrate the enhancement. One striking aspect of the fluorescence decay profiles is that the neat mechanism is still operative in the presence of the hydrocarbons. When acetylene, acetylene derivatives, and benzene were considered previously, the resulting decay profiles seemed to indicate an absence of the neat mechanism in the presence of the triplet mechanism. The discrepancy is attributed to the shorter pulse width and higher intensity of the excitation from the Nd:YAG laser employed in the present experiments.

For each set of chemiluminescence decay profiles acquired for a hydrocarbon/NO_2 mixture, a neat NO_2 decay profile was acquired for 10 Torr of NO_2 under identical conditions. This neat chemiluminescence was used to optimize laser/cell alignment and provided a scaling factor used for data collected at different times. In addition, the neat chemiluminescence was subtracted from the chemiluminescence of the mixture to determine the formation rate constants (apparent decay constants) pertaining only to the reactions between NO_2 and the hydrocarbon, as opposed to NO_2 alone. The formation rates for all the reaction mixtures listed in Table 1 were obtained by fitting the decay portion of the data to a single exponential function.

Table 1
Chemiluminescence formation rates

Hydrocarbon	[Hydrocarbon] (Torr)*	[NO_2] (Torr)*	k_1($\times 10^6$ s^{-1})
Benzene	10.0	10.0	7.93±0.08
	4.0	10.0	4.25±0.01
	3.0	10.0	4.19±0.01
	2.0	10.0	3.704±0.008
	1.0	10.0	3.142±0.008
Toluene	10.0	10.0	7.8±0.1
	5.1	10.0	5.84±0.09
	4.1	10.0	5.73±0.05
	3.0	10.0	5.05±0.04
	2.1	10.0	3.85±0.02
	1.0	10.0	3.44±0.02
Ethylbenzene	7.0	10.0	6.34±0.03
	5.5	10.0	8.54±0.08
	3.0	10.0	5.03±0.02
	2.0	10.0	4.29±0.02
	1.0	10.0	2.97±0.02
m-Xylene	5.0	10.0	3.07±0.01
	4.0	10.0	4.34±0.01
	3.0	10.0	3.13±0.01
	2.1	10.0	2.20±0.01
	1.0	10.0	1.88±0.01
o-Xylene	4.1	10.0	5.42±0.03
	3.0	10.0	2.92±0.01
	2.0	10.0	3.27±0.01
	1.0	10.0	2.65±0.03
p-Xylene	5.0	10.0	3.55±0.01
	4.0	10.0	3.10±0.01
	3.0	10.0	3.36±0.01
	2.0	10.0	5.7±0.2
	1.1	10.0	8.0±0.5

* The error in the pressure measurement is ±0.001 Torr.

For *m*- and *o*-xylenes, the general trend is an increase in the formation rate of NO(A) with an increase in hydrocarbon pressure. For *p*-xylenes the formation rate is larger or lower pressures. This seems ambiguous when compared to the other xylenes. Furthermore, a comparison of the xylenes indicates that *p*- and *m*-xylenes do not influence the NO(A) production rate as much as *o*-xylene.

Benzene, toluene, and ethylbenzene all exhibit formation rates greater than the rates for the xylenes at similar partial pressures which could result from the lesser degree of substitution about the benzene ring. One possibility is that the higher degree of substitution could affect the rate of $[NO_2 \cdots HC]^{**}$ complex dissociation. The lower formation rate for the xylenes may be attributed to steric hindrance of the two substituted methyl groups. No clear dependence of formation rates could be related to differences among the xylene isomers. Among the benzene derivatives, ethylbenzene is the benzene derivative that does not display a monotonic increase in the formation rate with increasing pressure, since its maximum formation rate is attained at 5.5 Torr.

The assumption of the triplet mechanism is based upon the participation of the hydrocarbon T_1 state in the enhancement of the NO fluorescence. Conversely, if the S_1 state of the hydrocarbons is directly excited via two-photon absorption, a different mechanism could be responsible for the ultimate production of excited NO. Using 532-nm irradiation, it is energetically possible to populate the triplet state of the hydrocarbon via two routes: (i) direct two-photon excitation of hydrocarbon singlet state and subsequent intersystem crossing to the triplet state; or (ii) two-photon excitation of $[NO_2 \cdots HC]$ followed by energy transfer to the hydrocarbon T_1 state. The excited singlet- and triplet-state energies of all the hydrocarbons are listed in Table 2. Considering the excitation wavelength of 532 nm, a single photon absorption would provide 2.3 eV of energy while a two-photon absorption would equal 4.6 eV. According to Table 2, a two-photon process would not be capable of exciting benzene directly to its S_1 state. Two photons would, however, provide enough energy for the NO_2/hydrocarbon complex to be excited above the T_1 state of all the hydrocarbons due to the absorption cross section of NO_2. Visible multiphoton excitation for NO_2 and, thus, $[NO_2 \cdots HC]^{**}$ is accomplished by a real intermediate state, since NO_2 has four low-lying coupled states that provide for a virtual continuous visible spectrum. The absorption cross section at 532 nm is $\sim 10^{-19}$ cm^2 molecule^{-1} [3]. The S_1 energies of the remainder of the compounds indicates that a two-photon absorption could directly excite these hydrocarbons to the S_1 state. The excitation spectrum of toluene in the $S_1 \leftarrow S_0$ region resulting from absorption of two visible photons has been observed previously [4]. Also, two-photon absorption by the xylenes in the visible region of the spectrum has been reported for the $S_1 \leftarrow S_0$ transition [5]. Even though toluene and the xylenes have been shown to be excited by two-photon absorption, the absorption cross sections of these compounds for the two-photon process are quite small [6], making this direct pathway to the S_1-hydrocarbon state improbable.

Table 2
Singlet state and triplet state energies of hydrocarbons (energies given in eV relative to ground state S_0)

Hydrocarbon	S_1 [5]	S_1 [6]	S_1 [7]	T_1 [5]	T_1 [7]
Benzene	4.8	4.8		3.7	
Toluene	4.6	4.6	4.6	3.6	3.5
Ethylbenzene			4.5		3.4
m-Xylene	4.6	4.6		3.5	
o-Xylene	4.6	4.6	4.5	3.5	3.4
p-Xylene	4.5	4.5	4.4	3.5	3.4

Visible two-photon absorption by NO_2 has been reported to proceed by near-resonant intermediate states [7]. A closely spaced system of real vibronic states attributed to three excited electronic-state origins lies at an energy nearly resonant with the one-photon energy [8]. With the absorption of the second photon the NO_2 molecule is promoted to the $^2B_2$ state and subsequent dissociation. For toluene, ethylbenzene, and the xylenes, the energy of one visible photon lies in the vibrational and rotational manifold well below the energy of the S_1 electronic state. Since no directly accessible energy states correspond to the one-photon energy, absorption of two photons would have to be simultaneous. Thus, with 532-nm excitation, the two-photon absorption cross section for NO_2 is expected to be greater than those of the hydrocarbons.

The lifetimes of the excited states of the hydrocarbons also tend to support the involvement of the T_1 state in the fluorescence enhancement. The lifetime of the S_1 state of toluene is ≈86 ns [9]. Following promotion to the S_1 state, intersystem crossing to the T_1 state is reported to occur at a rate of 8.5×10^6 s^{-1} at 37 500 cm^{-1} above the ground state [10]. The T_1 state lifetime of toluene is reported to be 2.9 ms at a pressure of 4×10^{-5} Torr. The data in Table 1 indicates that the lifetime for formation (k_1^{-1}) of NO($A^2\Sigma^+$) ranges from 128 to 291 ns for toluene. Comparing these lifetimes with those for the S_1 state, as well as the rate for intersystem crossing, it appears that any excitation of the S_1 state would relax in the very early stages of NO($A^2\Sigma^+$) formation, thus favoring the involvement of the hydrocarbon's long-lived T_1 state that is accessed by absorption of the NO_2/hydrocarbon complex.

The same arguments apply to ethylbenzene, which has an S_1 lifetime of 53 ns at its vapor pressure and which stretches to 80 ns when measured at 0.1 Torr [11]. Therefore, the NO($A^2\Sigma^+$) formation lifetime of NO for ethylbenzene spans 117–337 ns.

As a group, the xylenes follow the same pattern as toluene and ethylbenzene. For *o*-xylene, the S_1 lifetime is 52 ns [12], whereas the NO($A^2\Sigma^+$) formation lifetimes varies from 218 to 401 ns. The S_1 lifetime for *m*-xylene is 49 ns [12] with the range of NO($A^2\Sigma^+$) formation lifetimes ranging from 244 to 469 ns. Finally, for *p*-xylene the S_1 lifetime is 44 ns [12], in contrast to a NO($A^2\Sigma^+$) formation lifetime range of 285 to

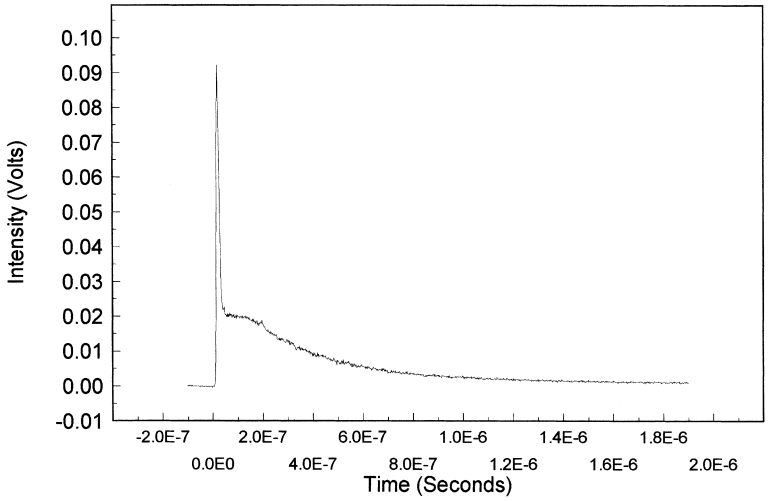

Fig. 3. Decay profile for 10-Torr NO_2 and 3-Torr acrylaldehyde.

137 ns. The triplet mechanism is founded upon the participation of the T_1 state of the hydrocarbons in the enhancement of $NO(A^2\Sigma^+)$ fluorescence. If the S_1 state of the hydrocarbons is directly excited via two photons, then a different mechanism could be responsible for the ultimate production of excited NO. However, based upon the low two-photon absorption cross sections and short S_1 lifetimes of toluene, ethylbenzene, and xylene, it appears that the triplet mechanism best accounts for the observed chemiluminescence.

Recent evidence that strengthens this triplet mechanism hypothesis is the observation made in this laboratory that of long-lived $NO(A^2\Sigma^+)$ chemiluminescence for the focused 532-nm irradiation of NO_2 and acrylaldehyde (acrolein, Fig. 3). Acrylaldehyde's structure is radically different from those of benzene and acetylene; however, it does possess a low-lying triplet state (T_1=3.01 eV) accessible via two 532-nm photons [13].

3.2. Dispersed emission

In an effort to attribute the observed chemiluminescence to the $NO(A^2\Sigma^+)\rightarrow NO(X^2\Pi)$ emission, a dispersed fluorescence spectrum was acquired.

Fig. 4 displays the dispersed fluorescence spectrum for a mixture consisting of 10 Torr of NO_2, 6 Torr of *p*-xylene, and 150 Torr of N_2 (added to suppress the excited rotational population of nitric oxide). A 450-ns wide boxcar gate was delayed 100 ns so that only the long-lived portion of the chemiluminescence was acquired, excluding emission from the neat mechanism. This spectrum is identified as the emis-

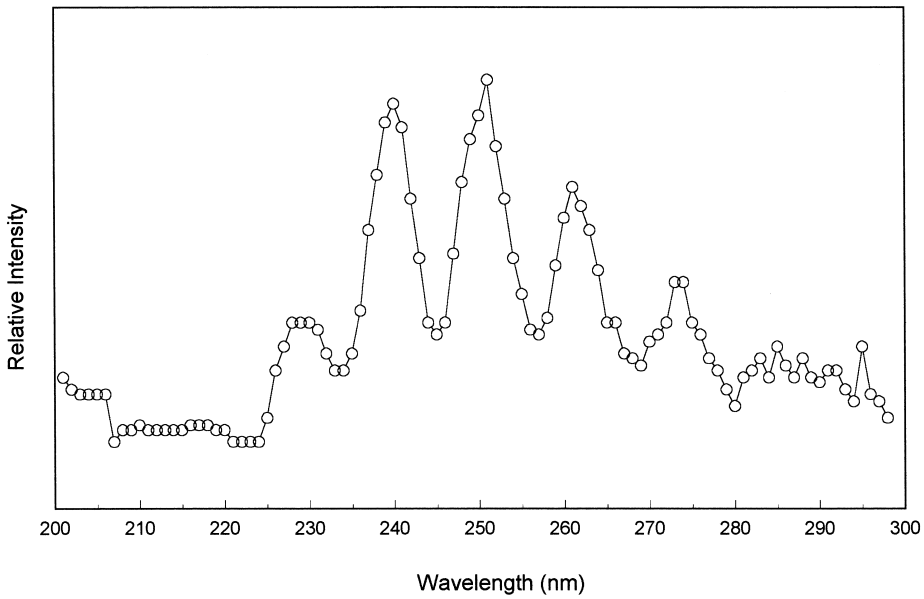

Fig. 4. Dispersed fluorescence of NO_2 and *p*-xylene.

sion spectrum of the γ-band of nitric oxide when compared to an assigned UV spectrum of NO [14].

The dispersed fluorescence spectrum of the NO_2/benzene was previously observed; thus NO_2/toluene and NO_2/ethylbenzene mixtures were not considered in this experiment due to their similarity to benzene. By the same reasoning, the isomeric nature of the xylenes suggests that, if the observed chemiluminescence for NO_2/*p*-xylene mixture results from $NO(A^2\Sigma^+) \rightarrow NO(X^2\Pi)$, the chemiluminescence for *m*- and *o*-xylenes with NO_2 is also from $NO(A^2\Sigma^+) \rightarrow NO(X^2\Pi)$.

3.3. *NO($A^2\Sigma^+$) quenching*

The formation rate constant, k_1 (Eq. (14)), was determined experimentally during the chemiluminescence studies, but the depletion rate constant, k_2, from Eq. (15) must be determined in another fashion.

Following the reaction between hydrocarbon and NO_2, the product, $NO(A^2\Sigma^+)$, relaxes to its ground state, $NO(X^2\Pi)$. The relaxation process can occur in several ways. One pathway is for $NO(A^2\Sigma^+)$ to relax through radiative emission. Other possibilities consist of $NO(A^2\Sigma^+)$ being quenched by collisions with NO_2 or the hydrocarbon that is in the reaction mixture. Since the concentration of nascent $NO(A^2\Sigma^+)$ changes as the reaction proceeds, as a result of 'bright' and 'dark' processes, the optical signal detected does not represent the total concentration of $NO(A^2\Sigma^+)$ produced in the reaction. The chemiluminescence observed represents only a fraction of the initial $NO(A^2\Sigma^+)$ present as a reaction product. The initial concentration of $NO(A^2\Sigma^+)$ must, therefore, be derived from the time integral of Eq. (17).

The experimentally observed quantity is the total fluorescence yield, Φ_{LLC}, defined by Eq. (18). This quantity corresponds to only a fraction of the concentration of the nascent $NO(A^2\Sigma^+)$, so it is desirable to relate these two quantities: Φ_{LLC} and nascent $[NO(A^2\Sigma^+)]$. In principle, the total depletion rate constant, k_2, can be determined by using the apparent formation rate constant. However, the temporal resolution of the present experiment is insufficient for determining the apparent formation rate constant. The depletion rate constant is defined as the sum of the rate constants for radiative emission, quenching by NO_2, and quenching by the hydrocarbon:

$$k_2 = k_f^0 + k_{NO_2}[NO_2] + k_{HC}[HC] \tag{19}$$

The ratio of observed $[NO(A^2\Sigma^+)]$ to the total nascent $[NO(A^2\Sigma^+)]_0$ amount can be related to the radiative rate constant divided by the total depletion rate constant:

$$\Phi_{LLC} = [NO(\tilde{A}^2\Sigma^+)]_0 \left(\frac{k_0^f}{k_f^0 + k_{NO_2}[NO_2] + k_{HC}[HC]} \right) \tag{20}$$

Substitution of Eq. (19) into Eq. (20) leads to:

$$[NO(\tilde{A}^2\Sigma^+)]_0 = (\text{const})\Phi_{LLC}k_2 \tag{21}$$

Since only relative values are of concern,

$$[NO(\tilde{A}^2\Sigma^+)]_0^{rel} = \Phi_{LLC}k_2 \tag{22}$$

Thus, the experimentally determined total fluorescence yield can be used along with the value of k_2 at each hydrocarbon pressure to calculate the relative concentration of nascent $NO(A^2\Sigma^+)$. Upon inspection of Eq. (19), all quantities are known except for the quenching rate constant for the hydrocarbon. Thus, quenching studies were conducted to obtain this value.

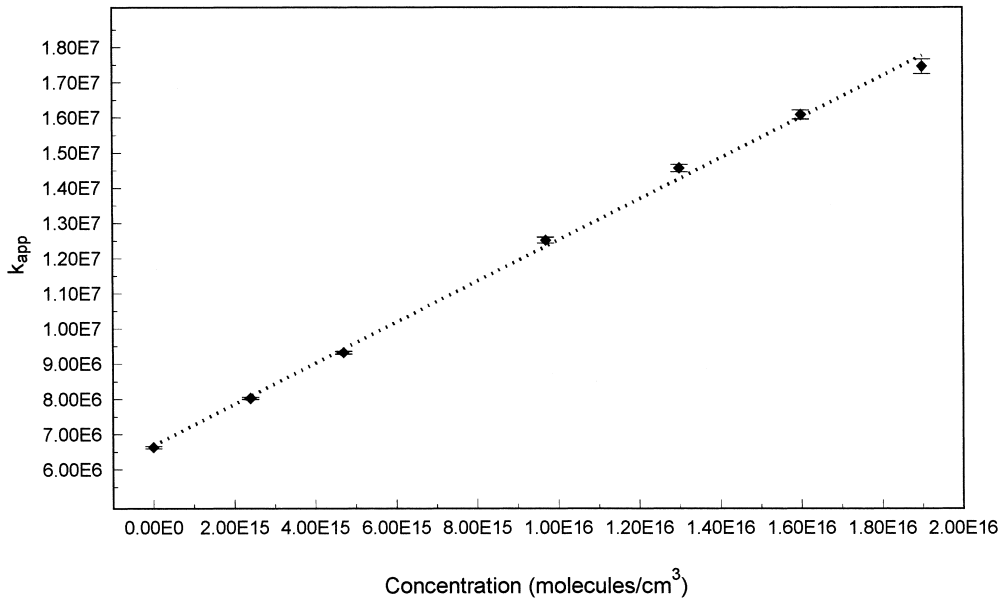

Fig. 5. Stern–Volmer plot for *m*-xylene.

Table 3
Hydrocarbon quenching rate constants

Hydrocarbon	k_{HC} ($\times 10^{-10}$ cm^3 molecule^{-1} s^{-1})
Benzene	6.0±0.4
Toluene	6.6±0.5
Ethylbenzene	4.7±0.5
m-Xylene	5.7±0.2
o-Xylene	5.6±0.4
p-Xylene	6.0±0.2

For a reaction mixture of a hydrocarbon and NO, a Stern–Volmer relation can be written.

$$k_{app} = k_f^0 + k_{NO}[NO] + k_{HC}[HC] \quad (23)$$

where, k_{app} is the observed fluorescence decay rate constant, k_{NO} the quenching rate constant of NO($A^2\Sigma^+$) by NO, and k_{HC} the quenching rate constant of the hydrocarbon. The fluorescence decay profiles for benzene, toluene, ethylbenzene, and the xylenes were obtained at various pressures while combining each with a constant pressure of NO. These decay profiles were fitted to a single exponential function, $I=I_0 \exp(-k_{app}t)$, to find the value for k_{app} at each hydrocarbon pressure. Fig. 5 is the Stern–Volmer plot that was constructed using the ([HC], k_{app})-data pairs from *m*-xylene with $\pm 2\sigma$ error bars. The k_{HC} values for *m*-xylene and the other hydrocarbons are shown in Table 3.

The NO($A^2\Sigma^+$) quenching rate constants for benzene and toluene were previously determined by Hass et al. [15] as $6.16\pm0.5\times10^{-10}$ and $5.45\pm0.5\times10^{-10}$ cm^3 molecule^{-1} s^{-1}, respectively. The value for benzene is consistent with our result within experimental error, whereas the value for toluene is 17% lower than our value. One possible reason for the discrepancy is that the present study measured the total UV emission from NO($A^2\Sigma^+$), whereas the previous study monitored the emission at 248 nm.

The quenching rate constant of toluene is anomalous in that it is the only benzene derivative whose quenching rate constant exceeds that of benzene. Since the molecular speed and the electron affinities of benzene derivatives are smaller than those of benzene [15], one might expect the values of the quenching rate constants to be smaller. This is the case for all derivatives except toluene. One other factor that needs to be considered in quenching is that of resonant energy transfer. All derivatives have energy levels that lie below the NO($A^2\Sigma^+$) state, thus pose as possible energy acceptors. Toluene's near-resonance energy transfer from NO($A^2\Sigma^+$) may proceed more efficiently than those of benzenes due to a higher density of states to offset the lower electron affinity and lower speed. From the quenching rate constants for the hydrocarbons, the depletion rate constants can be calculated from Eq. (23). The depletion rate constants are listed in Table 4 and were calculated using the determined k_{HC} values, namely 4.61×10^6 s^{-1} for k_f^0, and 3.72×10^{-10} cm^3 molecule^{-1} s^{-1} for k_{NO_2} [16,17].

Table 4
Chemiluminescence depletion rates

Hydrocarbon	[Hydrocarbon] (Torr)*	[NO_2] (Torr)*	k_2($\times 10^8$ s^{-1})
Benzene	10.0	10.0	3.2±0.1
	4.0	10.0	2.0±0.1
	3.0	10.0	1.8±0.1
	2.0	10.0	1.7±0.1
	1.0	10.0	1.5±0.1
Toluene	10.0	10.0	3.4±0.2
	5.1	10.0	2.4±0.1
	4.1	10.0	2.1±0.1
	3.0	10.0	1.9±0.1
	2.1	10.0	1.7±0.1
	1.0	10.0	1.5±0.1
Ethylbenzene	7.0	10.0	2.3±0.2
	5.5	10.0	2.1±0.2
	4.0	10.0	1.9±0.1
	3.0	10.0	1.7±0.1
	2.0	10.0	1.6±0.1
	1.0	10.0	1.4±0.1
m-Xylene	5.0	10.0	2.2±0.1
	4.0	10.0	2.0±0.1
	3.0	10.0	1.8±0.1
	2.1	10.0	1.7±0.1
	1.0	10.0	1.4±0.1
o-Xylene	4.1	10.0	2.0±0.1
	3.0	10.0	1.8±0.1
	2.0	10.0	1.6±0.1
	1.0	10.0	1.4±0.1
p-Xylene	5.0	10.0	2.2±0.1
	4.0	10.0	2.0±0.1
	3.0	10.0	1.8±0.1
	2.0	10.0	1.7±0.1
	1.1	10.0	1.5±0.1

* The error in the pressure measurement is ±0.001 Torr.

3.4. NO($A^2\Sigma^+$) yields

Using the data from the chemiluminescence experiments, chemiluminescence reaction yields were calculated. The yields combine both the short-time portion of the decay profile as well as the long-lived chemiluminescence intensity. Both are used in the evaluation of the reaction yields in an effort to illustrate the increase in the reaction yield upon hydrocarbon addition.

Both the chemiluminescence yields and the calculated relative nascent yields are shown in Fig. 6 for the benzene derivatives and in Fig. 7 for the xylenes. The actual yields have been normalized with respect to the neat NO_2 system yield.

It is noteworthy that, for benzene, toluene, and ethylbenzene, the chemiluminescence yields attain a maximum at a low hydrocarbon pressure. In contrast, the NO($A^2\Sigma^+$) yields tend toward a minimum at low hydrocarbon pressures. Initially, the chemiluminescence yield increases with increasing hydrocarbon pressures; however, at high pressures the chemiluminescence yield decreases. The reason for this behavior of chemiluminescence yield is due to competition

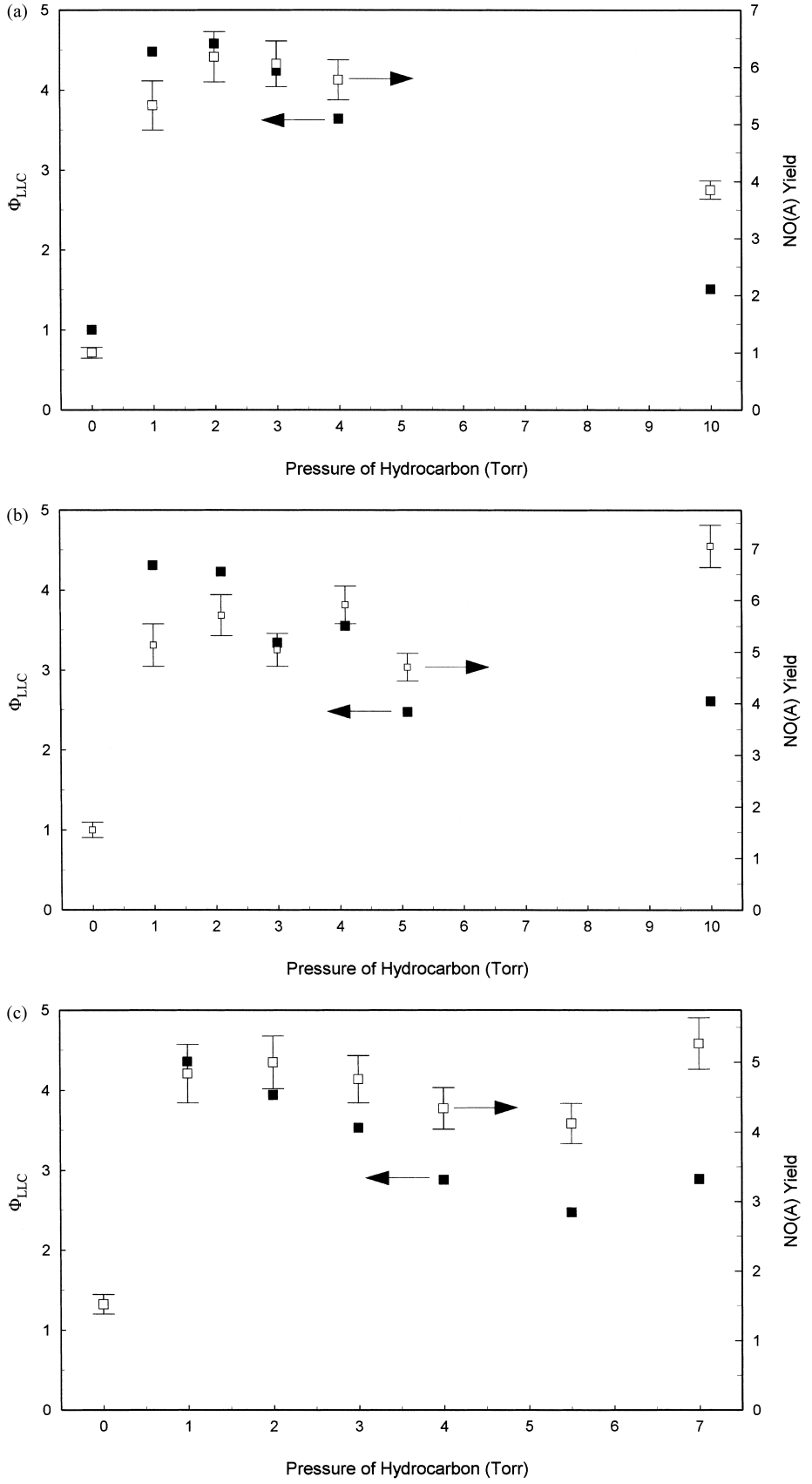

Fig. 6. (a) Reaction yields for benzene; (b) reaction yields for toluene; and (c) reaction yields for ethylbenzene.

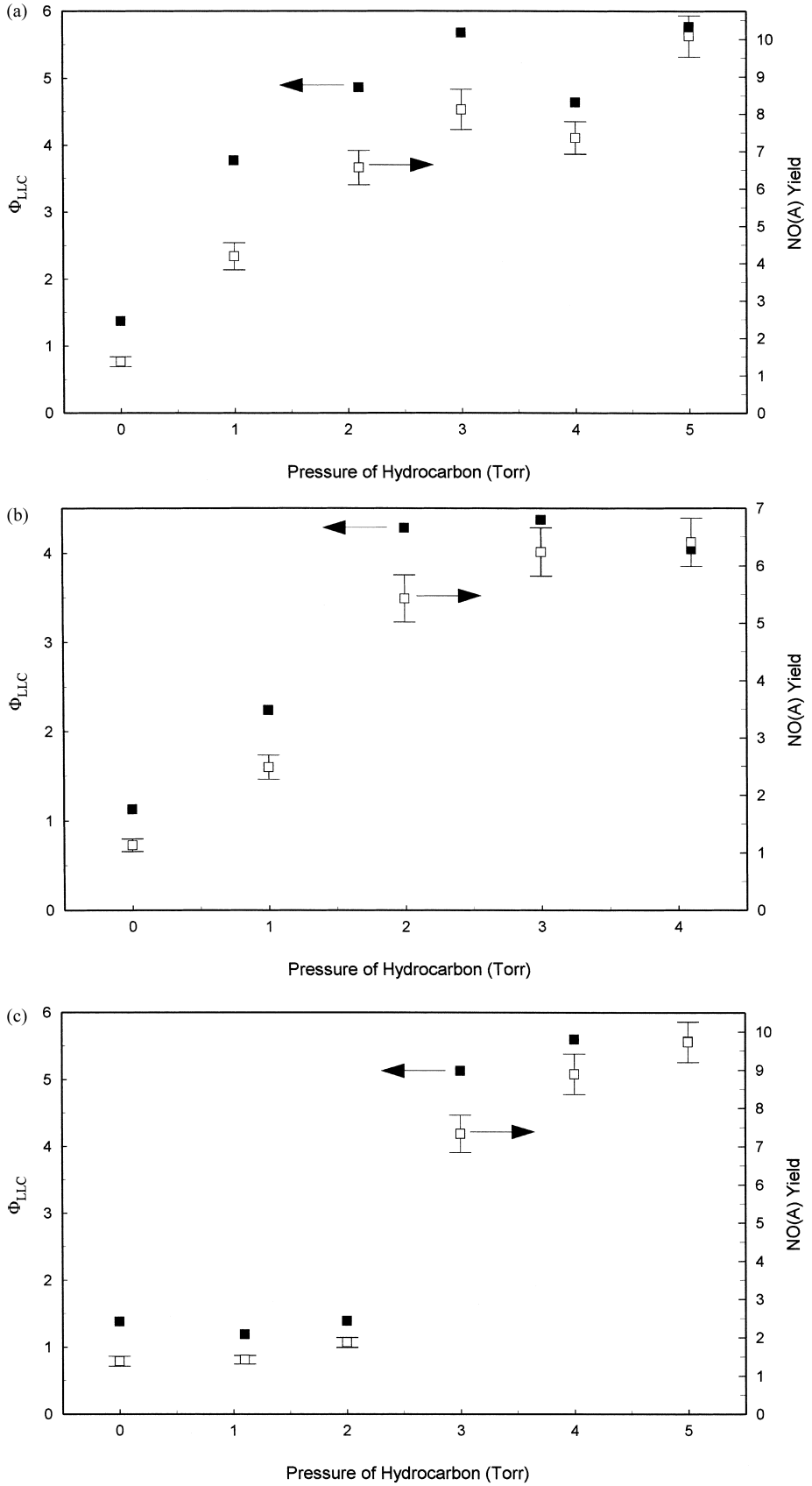

Fig. 7. (a) Reaction yields for *m*-xylene; (b) reaction yields for *o*-xylene; and (c) reaction yields for *p*-xylene.

between the hydrocarbon's ability to promote production of $[NO(A^2\Sigma^+)]_0$ and its ability to collisionally quench the $NO(A^2\Sigma^+)$. At the lower pressures as the hydrocarbon aids in producing $[NO(A^2\Sigma^+)]_0$ and chemiluminescence, the concentration of hydrocarbon in the reaction mixture is sufficiently low resulting in a low collision frequency, enabling nitric oxide to fluoresce rather than collisionally deactivate. As the pressure of the hydrocarbon is increased the relative chemiluminescence yield decreases, because the excited nitric oxide is quenched at a greater rate due to the higher concentration of hydrocarbon. Again, notice that as the hydrocarbon pressure is increased, the relative amount of $[NO(A^2\Sigma^+)]_0$ produced tends to increase, since the hydrocarbon is aiding in the production of $[NO(A^2\Sigma^+)]_0$. Recall in the triplet mechanism that the hydrocarbon is needed to produce $NO(A^2\Sigma^+)$, so the presence of more hydrocarbon should result in a larger nascent $NO(A^2\Sigma^+)$ yield. This is an oversimplification, since the hydrocarbon may also quench $NO_2(^2B_2)$, but $NO_2^{(*)}$ is able to undergo many collisions and yet maintain a significant amount of internal energy [18].

The question of enhancement efficiency for the hydrocarbons can also be answered by comparing the magnitude of the yields. For all six species, the maximum relative Φ_{LLC} values fall between 4 and 6 units. For benzene, toluene, and ethylbenzene, the enhancement efficiency is approximately the same. Likewise, the $NO(A^2\Sigma^+)$ yields appear to be approximately equal when the range of hydrocarbon pressures are considered. Within the accessible hydrocarbon range for the xylenes, the Φ_{LLC} values are comparable to those for benzene, toluene, and ethylbenzene, but it must be emphasized again that the pressure of maximum efficiency is not known. It is possible that the chemiluminescence intensity could be much greater than that observed in this study.

The $[NO(A^2\Sigma^+)]_0$ yields for the xylenes are not in the same range as the benzene derivatives. If the same pressure ranges (3–4 Torr) are considered for these compounds, the $[NO(A)]_0$ yields for the xylenes exceed that of any of the benzene derivatives. However, as stated earlier, the xylene formation rates are lower than the formation rates for the benzene derivatives and the depletion rates are equal. Thus, based on these rate constants, one would expect Φ_{LLC} $[NO(A^2\Sigma^+)]_0$ yields for xylene to be lower than those of the benzene derivatives. Observation runs contrary to this, suggesting a difference of interaction time, i.e. the chemiluminescence reactions for the xylenes are of longer duration, albeit of lower formation rate. One way in which the observed rate constants may lead to the observed yields for Φ_{LLC} $[NO(A^2\Sigma^+)]_0$ is by the following scheme for $[NO(A^2\Sigma^+)]$ formation. Suppose the yield of $[NO_2 \cdots HC]^{**}$ is higher for xylenes than benzene derivatives, and the rate limiting step for [NO(A)] production is that of $[NO_2 \cdots HC]^{**}$ dissociation and/or $NO_2{}^{(*)}+HC(T_1)$ reaction (Eqs. (6) and (9)). If this rate limiting step is faster for the benzene derivatives compared to the xylenes, this would lead to higher yields for xylenes despite the lower formation rate. This is possible because the lower $[NO_2^{(*)}]$ and $[HC^*(T_1)]$ steady-state values may persist longer due to the higher $[NO_2 \cdots HC(T_1)]^{**}$yield. This reinforces the fact that the formation rate constant does not correspond to an elementary reaction, but rather it is an overall rate constant.

Possible factors that could influence the variation in $[NO(A^2\Sigma^+)]_0$ yields include the degree of complex formation, the quenching of NO_2 ($^2B_2$) by the hydrocarbon, and the efficiency of energy transfer from $NO_2^{(*)}$ to $HC(T_1)$ within the excited complex.

4. Conclusions

Visible laser irradiation of HC/NO_2 mixtures, where HC represents toluene, ethylbenzene, and the xylene isomers, produced ultraviolet chemiluminescence. The chemiluminescence of the mixture was enhanced relative to that of neat NO_2. The origin of the enhanced chemiluminescence was shown to arise from relaxation of $NO(A^2\Sigma^+)$ by recording the dispersed emission spectrum. A comparison of chemiluminescence yields at the same pressures show the xylenes to be more efficient in NO(A) production than the benzene derivatives, although the chemiluminescence formation rates for xylenes were significantly lower. This is attributed to longer reaction lifetimes due to the complex $NO(A^2\Sigma^+)$ production mechanism. No significant difference was observed in the chemilumiscence or $NO(A^2\Sigma^+)$ yields between the xylene isomers. This observed chemiluminescence was explained by the triplet mechanism. Support for this mechanism was bolstered by the observation of NO γ-band emission following the focused 532-nm irradiation of acrylaldehyde.

Acknowledgements

The authors would like to thank Dr. Jordan C. Poler, Dr. Daniel S. Jones, and Dr. M. Yasin Akhtar Raja.

References

[1] Y. Fujimura, K. Honma, O. Kajimoto, Chem. Phys. Lett. 140 (1987) 320.
[2] W. Sisk, H. Endo, K. Shibuya, J. Phys. Chem. 96 (1992) 6668.
[3] H.S. Johnston, C.E. Miller, B.Y. Oh, K.O. Patten Jr., W.N. Sisk, J. Phys. Chem. 97 (1993) 9890.
[4] R. Vasudev, J.C.D. Brand, Chem. Phys. 37 (1979) 211.
[5] T.G. Blease, R.J. Donovan, P.R.R. Langridge-Smith, T. Ridley, Laser Chem. 9 (1988) 241.
[6] C.H. Chen, M.P. McCann, J. Chem. Phys. 88 (1988) 4671.
[7] L. Bigio, E.R. Grant, Isr. J. Chem. 24 (1984) 251.
[8] L. Bigio, R.S. Tapper, E.R. Grant, J. Phys. Chem. 88 (1984) 1271.
[9] C.G. Hickman, J.R. Gascooke, W.D. Lawrance, J. Chem. Phys. 104 (1996) 4887.
[10] B.M. Toselli, J.D. Brenner, M.L. Yerram, W.E. Chin, K.D. King, J.R. Barker, J. Chem. Phys. 95 (1991) 176.
[11] J. Prochorow, W. Hopewell, M.A. El-Sayed, Chem. Phys. Lett. 65 (1979) 410.

[12] G.M. Breuer, E.K.C. Lee, Chem. Phys. Lett. 14 (1972) 404.
[13] J.C.D. Brand, D.G. Williamson, Discussions Fraraday Soc. 35 (1963) 184.
[14] J. Danielak, U. Domin, R. Kepa, M. Rytel, M. Zachwieja, J. Mol. Spectrosc. 181 (1997) 394.
[15] Y. Hass, G.D. Greenblatt, J. Phys. Chem. 90 (1986) 513.
[16] S. McDermid, J.B. Laudenslager, J. Quant. Spectrosc. Radiat. Transfer 27 (1982) 1.
[17] M. Asscher, Y. Haas, J. Chem. Phys. 76 (1982) 2115.
[18] K.O. Patten Jr., J.D. Burley, H.S. Johnston, J. Chem. Phys. 85 (1986) 7146.